Hindawi Publishing Corporation
EURASIP Journal on Wireless Communications and Networking
Volume 2009, Article ID 302092, 10 pages
doi:10.1155/2009/302092

Review Article

MIMO Technologies in 3GPP LTE and LTE-Advanced

Juho Lee,[1] Jin-Kyu Han,[1] and Jianzhong (Charlie) Zhang[2]

[1] *Digital Media & Communications R&D Center, Samsung Electronics, 416, Maetan-3dong, Yeongtong-gu, Suwon-si 443-742, South Korea*
[2] *Wireless System Lab, Samsung Telecom America, 1301 E. Lookout Drive, Richardson, TX 75082, USA*

Correspondence should be addressed to Juho Lee, juho95.lee@samsung.com

Received 13 February 2009; Accepted 31 May 2009

Recommended by Angel Lozano

3rd Generation Partnership Project (3GPP) has recently completed the specification of the Long Term Evolution (LTE) standard. Majority of the world's operators and vendors are already committed to LTE deployments and developments, making LTE the market leader in the upcoming evolution to 4G wireless communication systems. Multiple input multiple output (MIMO) technologies introduced in LTE such as spatial multiplexing, transmit diversity, and beamforming are key components for providing higher peak rate at a better system efficiency, which are essential for supporting future broadband data service over wireless links. Further extension of LTE MIMO technologies is being studied under the 3GPP study item "LTE-Advanced" to meet the requirement of IMT-Advanced set by International Telecommunication Union Radiocommunication Sector (ITU-R). In this paper, we introduce various MIMO technologies employed in LTE and provide a brief overview on the MIMO technologies currently discussed in the LTE-Advanced forum.

1. Introduction

As multimedia communications become increasingly popular, mobile communications are expected to reliably support high data rate transmissions. Multiple input multiple output (MIMO) has been treated as an emerging technology to meet the demand for higher data rate and better cell coverage even without increasing average transmit power or frequency bandwidth, since it was proved that MIMO structure successfully constructs multiple spatial layers where multiple data streams are delivered on a given frequency-time resource and linearly increases the channel capacity [1–8]. Lots of recently specified wireless communications standards are ready to support MIMO technologies.

3rd Generation Partnership Project (3GPP) has recently specified an Orthogonal Frequency Division Multiplexing (OFDM) based technology, Evolved Universal Terrestrial Radio Access (E-UTRA), for support of wireless broadband data service up to 300 Mbps in the downlink and 75 Mbps in the uplink [9]. (E-UTRA is also known as LTE in the wireless industry.) In Long Term Evolution (LTE), MIMO technologies have been widely used to improve downlink peak rate, cell coverage, as well as average cell throughput.

To achieve this diverse set of objectives, LTE adopted various MIMO technologies including transmit diversity, single user (SU)-MIMO, multiuser (MU)-MIMO, closed-loop rank-1 precoding, and dedicated beamforming [10–13]. The SU-MIMO scheme is specified for the configuration with two or four transmit antennas in the downlink, which supports transmission of multiple spatial layers with up to four layers to a given User Equipment (UE). The transmit diversity scheme is specified for the configuration with two or four transmit antennas in the downlink, and with two transmit antennas in the uplink. The MU-MIMO scheme allows allocation of different spatial layers to different users in the same time-frequency resource, and is supported in both uplink and downlink. The closed-loop rank-1 precoding scheme is used to improve data coverage utilizing SU-MIMO technology based on the cell-specific common reference signal while introducing a control signal message that has lower overhead. The dedicated beamforming scheme is used for data coverage extension when the data demodulation based on dedicated reference signal is supported by the UE.

A study item called "LTE-Advanced" has recently started in 3GPP, with the goal of providing a competitive IMT-Advanced candidate proposal with accompanying

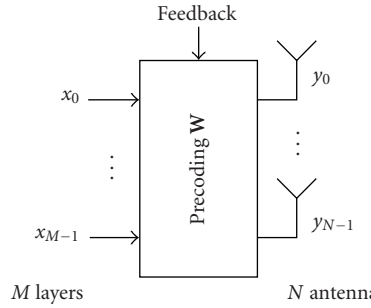

Figure 1: Closed-loop spatial multiplexing with N antennas and M layers.

Table 1: Precoding codebook for transmission on two antennas.

Codebook index	Number of layers M	
	1	2
0	$\frac{1}{\sqrt{2}}\begin{bmatrix}1\\1\end{bmatrix}$	—
1	$\frac{1}{\sqrt{2}}\begin{bmatrix}1\\-1\end{bmatrix}$	$1/2\begin{bmatrix}1&1\\1&-1\end{bmatrix}$
2	$\frac{1}{\sqrt{2}}\begin{bmatrix}1\\j\end{bmatrix}$	$1/2\begin{bmatrix}1&1\\j&-j\end{bmatrix}$
3	$\frac{1}{\sqrt{2}}\begin{bmatrix}1\\-j\end{bmatrix}$	—

self-evaluation results for the submission to International Telecommunication Union Radiocommunication Sector (ITU-R) in October 2009 [14]. In LTE-Advanced, the existing SU-MIMO technologies are extended to support configuration with up to eight transmit antennas in the downlink, and up to four transmit antennas in the uplink. In addition, multicell coordinated multipoint transmission (COMP) are also under active discussion and evaluation [15].

In this paper, we introduce various MIMO technologies employed in LTE, and provide a brief overview on the MIMO technologies currently discussed in the LTE-Advanced forum.

2. Downlink SU-MIMO in LTE

The SU-MIMO scheme is applied to the Physical Downlink Shared Channel (PDSCH), which is the physical layer channel that carries the information data from the network to the UE. With SU-MIMO spatial multiplexing, the LTE system provides a peak rate of 150 Mbps for two transmit antennas and 300 Mbps for four transmit antennas [16]. There are two operation modes in SU-MIMO spatial multiplexing: the closed-loop spatial multiplexing mode and the open-loop spatial multiplexing mode.

In the closed-loop spatial multiplexing mode, the base station (also known as eNodeB) applies the spatial domain precoding on the transmitted signal taking into account the precoding matrix indicator (PMI) reported by the UE so that the transmitted signal matches with the spatial channel experienced by the UE. The closed-loop spatial multiplexing with M layers and N transmit antennas ($N \geq M$) is illustrated in Figure 1. To support the closed-loop spatial multiplexing in the downlink, the UE needs to feedback the rank indicator (RI), the PMI, and the channel quality indicator (CQI) in the uplink. The RI indicates the number of spatial layers that can be supported by the current channel experienced at the UE. The eNodeB may decide the transmission rank, M, taking into account the RI reported by the UE as well as other factors such as traffic pattern, available transmission power, etc. The CQI feedback indicates a combination of modulation scheme and channel coding rate that the eNodeB should use to ensure that the block error probability experienced at the UE will not exceed 10%.

The precoding operation for the closed-loop spatial multiplexing is defined by

$$\mathbf{y} = \mathbf{W}\mathbf{x}, \tag{1}$$

where $\mathbf{y} = [y_0, \ldots, y_{N-1}]^T$, $\mathrm{y_n}$ denotes the complex symbol transmitted on the nth antenna, $\mathbf{x} = [x_0, \ldots, x_{M-1}]^T$, $\mathrm{x_m}$ denotes the modulation symbol transmitted on the mth layer, and $\mathbf{W}$ denotes the $N \times M$ precoding matrix. For transmission on two antennas, the precoding matrix $\mathbf{W}$ is selected from Table 1, where each column vector is in the form of $[\,1 \; e^{j(\theta+k\pi)}\,]^T$ multiplied by a scaling factor. For transmission on four antennas, the precoding matrix $\mathbf{W}$ is selected from Table 2, where $\mathbf{W}_i^{\{c_1 \ldots c_m\}}$ denotes the matrix defined by the columns $c_1, \ldots, c_m$ of the matrix $\mathbf{W}_i = \mathbf{I}_{4\times 4} - 2\mathbf{u}_i\mathbf{u}_i^H/\mathbf{u}_i^H\mathbf{u}_i$. Design of the precoding for four transmit antennas is based on the Householder transformation [17] to reduce the computational complexity at the UE as well as the design complexity for finding out suitable precoding matrices due to its structure. Note that the downlink reference signal is common for all UEs belonging to the cell and hence is not precoded by $\mathbf{W}$. The UE receives the information from the eNodeB on what precoding matrix is used, which is utilized by the UE for demodulating the data.

The precoding codebook was designed to satisfy the following properties.

Constant modulus. All physical transmit antennas keep the same transmit power level regardless which precoding matrix is used to maximize the power amplifier utilization efficiency.

Nested property. Each precoding matrix in a higher rank subcodebook can find at least one precoding matrix in a lower rank subcodebook, which is a submatrix of the higher rank precoding matrix. This property is included to ensure proper performance when the eNodeB overrides the RI report and decides on a transmission rank that is lower than the channel rank reported in the RI. This property also helps reduce the CQI calculation complexity as some of the precoding matrix selection procedures can be shared among precoding matrices designed for different transmission ranks. For example, in Table 2, for the precoding matrix with codebook index 0 in M = 3 subcodebook, $\mathbf{W}_0^{\{124\}}/\sqrt{3}$, we can find a precoding matrix with codebook index 0 in $M = 2$ subcodebook, $\mathbf{W}_0^{\{14\}}/\sqrt{2}$, which is a submatrix of $\mathbf{W}_0^{\{124\}}/\sqrt{3}$ (up to power scaling).

Table 2: Precoding codebook for transmission on four antennas.

Codebook index	$\mathbf{u}_i$	Number of layers M			
		1	2	3	4
0	$\mathbf{u}_0 = [1\ -1\ -1\ -1]^T$	$\mathbf{W}_0^{\{1\}}$	$\mathbf{W}_0^{\{14\}}/\sqrt{2}$	$\mathbf{W}_0^{\{124\}}/\sqrt{3}$	$\mathbf{W}_0^{\{1234\}}/2$
1	$\mathbf{u}_1 = [1\ -j\ 1\ j]^T$	$\mathbf{W}_1^{\{1\}}$	$\mathbf{W}_1^{\{12\}}/\sqrt{2}$	$\mathbf{W}_1^{\{123\}}/\sqrt{3}$	$\mathbf{W}_1^{\{1234\}}/2$
2	$\mathbf{u}_2 = [1\ 1\ -1\ 1]^T$	$\mathbf{W}_2^{\{1\}}$	$\mathbf{W}_2^{\{12\}}/\sqrt{2}$	$\mathbf{W}_2^{\{123\}}/\sqrt{3}$	$\mathbf{W}_2^{\{3214\}}/2$
3	$\mathbf{u}_3 = [1\ j\ 1\ -j]^T$	$\mathbf{W}_3^{\{1\}}$	$\mathbf{W}_3^{\{12\}}/\sqrt{2}$	$\mathbf{W}_3^{\{123\}}/\sqrt{3}$	$\mathbf{W}_3^{\{3214\}}/2$
4	$\mathbf{u}_4 = [1\ (-1-j)/\sqrt{2}\ -j\ (1-j)/\sqrt{2}]^T$	$\mathbf{W}_4^{\{1\}}$	$\mathbf{W}_4^{\{14\}}/\sqrt{2}$	$\mathbf{W}_4^{\{124\}}/\sqrt{3}$	$\mathbf{W}_4^{\{1234\}}/2$
5	$\mathbf{u}_5 = [1\ (1-j)/\sqrt{2}\ j\ (-1-j)/\sqrt{2}]^T$	$\mathbf{W}_5^{\{1\}}$	$\mathbf{W}_5^{\{14\}}/\sqrt{2}$	$\mathbf{W}_5^{\{124\}}/\sqrt{3}$	$\mathbf{W}_5^{\{1234\}}/2$
6	$\mathbf{u}_6 = [1\ (1+j)/\sqrt{2}\ -j\ (-1+j)/\sqrt{2}]^T$	$\mathbf{W}_6^{\{1\}}$	$\mathbf{W}_6^{\{13\}}/\sqrt{2}$	$\mathbf{W}_6^{\{134\}}/\sqrt{3}$	$\mathbf{W}_6^{\{1324\}}/2$
7	$\mathbf{u}_7 = [1\ (-1+j)/\sqrt{2}\ j\ (1+j)/\sqrt{2}]^T$	$\mathbf{W}_7^{\{1\}}$	$\mathbf{W}_7^{\{13\}}/\sqrt{2}$	$\mathbf{W}_7^{\{134\}}/\sqrt{3}$	$\mathbf{W}_7^{\{1324\}}/2$
8	$\mathbf{u}_8 = [1\ -1\ 1\ 1]^T$	$\mathbf{W}_8^{\{1\}}$	$\mathbf{W}_8^{\{12\}}/\sqrt{2}$	$\mathbf{W}_8^{\{124\}}/\sqrt{3}$	$\mathbf{W}_8^{\{1234\}}/2$
9	$\mathbf{u}_9 = [1\ -j\ -1\ -j]^T$	$\mathbf{W}_9^{\{1\}}$	$\mathbf{W}_9^{\{14\}}/\sqrt{2}$	$\mathbf{W}_9^{\{134\}}/\sqrt{3}$	$\mathbf{W}_9^{\{1234\}}/2$
10	$\mathbf{u}_{10} = [1\ 1\ 1\ -1]^T$	$\mathbf{W}_{10}^{\{1\}}$	$\mathbf{W}_{10}^{\{13\}}/\sqrt{2}$	$\mathbf{W}_{10}^{\{123\}}/\sqrt{3}$	$\mathbf{W}_{10}^{\{1324\}}/2$
11	$\mathbf{u}_{11} = [1\ j\ -1\ j]^T$	$\mathbf{W}_{11}^{\{1\}}$	$\mathbf{W}_{11}^{\{13\}}/\sqrt{2}$	$\mathbf{W}_{11}^{\{134\}}/\sqrt{3}$	$\mathbf{W}_{11}^{\{1324\}}/2$
12	$\mathbf{u}_{12} = [1\ -1\ -1\ 1]^T$	$\mathbf{W}_{12}^{\{1\}}$	$\mathbf{W}_{12}^{\{12\}}/\sqrt{2}$	$\mathbf{W}_{12}^{\{123\}}/\sqrt{3}$	$\mathbf{W}_{12}^{\{1234\}}/2$
13	$\mathbf{u}_{13} = [1\ -1\ 1\ -1]^T$	$\mathbf{W}_{13}^{\{1\}}$	$\mathbf{W}_{13}^{\{13\}}/\sqrt{2}$	$\mathbf{W}_{13}^{\{123\}}/\sqrt{3}$	$\mathbf{W}_{13}^{\{1324\}}/2$
14	$\mathbf{u}_{14} = [1\ 1\ -1\ -1]^T$	$\mathbf{W}_{14}^{\{1\}}$	$\mathbf{W}_{14}^{\{13\}}/\sqrt{2}$	$\mathbf{W}_{14}^{\{123\}}/\sqrt{3}$	$\mathbf{W}_{14}^{\{3214\}}/2$
15	$\mathbf{u}_{15} = [1\ 1\ 1\ 1]^T$	$\mathbf{W}_{15}^{\{1\}}$	$\mathbf{W}_{15}^{\{12\}}/\sqrt{2}$	$\mathbf{W}_{15}^{\{123\}}/\sqrt{3}$	$\mathbf{W}_{15}^{\{1234\}}/2$

Constrained alphabet. In case of two transmit antennas, constructing the precoding matrices by only using QPSK alphabet $\{\pm 1, \pm j\}$ except the scaling factor of $1/\sqrt{2}$ or 1/2 avoids the need for matrix multiplication in applying the precoder to the channel matrix without significant loss in precoding performance. In case of four transmit antennas, on the other hand, the QPSK alphabet constraint turns out to be a limiting factor in achieving additional spectral efficiency gain from additional antennas. It is also noted that if the Minimum Mean Squared Error (MMSE) receiver is assumed, most of the computational burden for CQI calculation comes from the matrix multiplication required to inverse the instantaneous covariance matrix and not from the multiplication of the channel matrix and the precoder. Taking into account these aspects, 8-PSK alphabet $\{\pm 1, \pm j, \pm(1+j)/\sqrt{2}, \pm(-1+j)/\sqrt{2}\}$ is used for the elements of vector $\mathbf{u}_i$ as a tradeoff between the computational complexity and the achievable performance of the codebook designed for four transmit antenna.

For the spatial multiplexing, multiple codewords may be mapped to multiple layers depending on the transmission rank scheduled by the eNodeB. In the LTE downlink, hybrid automatic repeat request (HARQ) process is operated for each codeword. Each HARQ process requires an ACK/NAK feedback signaling on uplink. To reduce the uplink feedback overhead, only up to two codewords are transmitted even though more than two layers can be transmitted on downlink in a given subframe, giving rise to the need of defining a rule for mapping a codeword to its layers. In LTE, codewords are mapped to layers according to Table 3, where $d_k(i)$ denotes the ith modulation symbol of the kth codeword, $x_l(i)$ denotes the ith modulation symbol of the lth layer, S_{layer} denotes the number of modulation symbols of each layer, and S_{k} denotes the number of modulation symbols of the kth codeword. If there is one layer, there is one codeword. If there are two layers, the basic mode of operation is to carry a codeword for each layer. The case of transmitting a single codeword using two layers is only applicable for the eNodeB having four transmit antennas when its initial transmission contained two codewords and a codeword mapped onto two layers needs to be retransmitted. In case of three-layer transmission, the first layer carry the first codeword while the second and the third layers carries the second codeword, in which case the second codeword has two times modulation symbols than the first one. When four layers are scheduled, two codewords are transmitted, each of which is transmitted using two layers. As can be seen in Table 3, the modulation symbols of a codeword are equally split into two layers when the codeword is mapped to two layers.

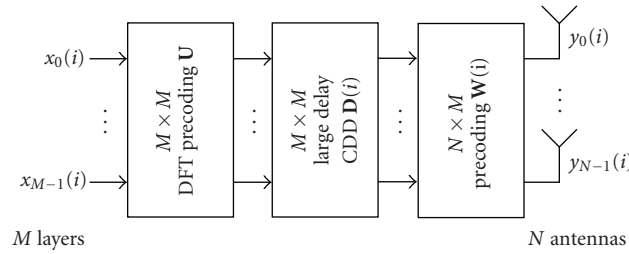

Figure 2: Open-loop spatial multiplexing with N antennas and M layers.

For the closed-loop spatial multiplexing, the eNodeB sends the scheduled UE the information about what precoding matrix is used as a part of downlink control information, using a three-bit information field for two transmit antennas and a six-bit information field for four transmit antennas. This information field is denoted transmit precoding matrix indication (TPMI). To support frequency-selective

Table 3: Codeword-to-layer mapping for spatial multiplexing.

Number of layers	Number of codewords	Codeword-to-layer mapping $i = 0, 1, \ldots, S_{layer} - 1$	
1	1	$x_0(i) = d_0(i)$	$S_{layer} = S_0$
2	2	$x_0(i) = d_0(i)$ $x_1(i) = d_1(i)$	$S_{layer} = S_0 = S_1$
2	1	$x_0(i) = d_0(2i)$ $x_1(i) = d_0(2i+1)$	$S_{layer} = S_0/2$
3	2	$x_0(i) = d_0(i)$ $x_1(i) = d_1(2i)$ $x_2(i) = d_1(2i+1)$	$S_{layer} = S_0 = S_1/2$
4	2	$x_0(i) = d_0(2i)$ $x_1(i) = d_0(2i+1)$ $x_2(i) = d_1(2i)$ $x_3(i) = d_1(2i+1)$	$S_{layer} = S_0/2 = S_1/2$

Table 4: DFT precoding matrix $\mathbf{U}$.

Number of layers M	M × M matrix $\mathbf{U}$
2	$\frac{1}{\sqrt{2}}\begin{bmatrix} 1 & 1 \\ 1 & e^{-j2\pi/2} \end{bmatrix}$
3	$\frac{1}{\sqrt{3}}\begin{bmatrix} 1 & 1 & 1 \\ 1 & e^{-j2\pi/3} & e^{-j4\pi/3} \\ 1 & e^{-j4\pi/3} & e^{-j8\pi/3} \end{bmatrix}$
4	$\frac{1}{2}\begin{bmatrix} 1 & 1 & 1 & 1 \\ 1 & e^{-j2\pi/4} & e^{-j4\pi/4} & e^{-j6\pi/4} \\ 1 & e^{-j4\pi/4} & e^{-j8\pi/4} & e^{-j12\pi/4} \\ 1 & e^{-j6\pi/4} & e^{-j12\pi/4} & e^{-j18\pi/4} \end{bmatrix}$

Table 5: Large delay CDD matrix $\mathbf{D}(i)$.

Number of layers M	$\mathbf{D}(i)$
2	$\begin{bmatrix} 1 & 0 \\ 0 & e^{-j2\pi i/2} \end{bmatrix}$
3	$\begin{bmatrix} 1 & 0 & 0 \\ 0 & e^{-j2\pi i/3} & 0 \\ 0 & 0 & e^{-j4\pi i/3} \end{bmatrix}$
4	$\begin{bmatrix} 1 & 0 & 0 & 0 \\ 0 & e^{-j2\pi i/4} & 0 & 0 \\ 0 & 0 & e^{-j4\pi i/4} & 0 \\ 0 & 0 & 0 & e^{-j6\pi i/4} \end{bmatrix}$

precoding without excessive downlink signaling overhead, the TPMI can also indicate that the precoding matrices reported in the most recent PMI report from the scheduled UE are used for their corresponding frequency resources. If the TPMI indicates a precoding matrix, the indicated precoding matrix is applied to all frequency resources allocated. In order to cope with the situation that the spatial multiplexing is not possible due to channel variation, the eNodeB can instantaneously schedule downlink transmission using the transmit diversity even though the UE has been configured to be in the spatial multiplexing mode. Use of the transmit diversity is indicated by TPMI.

Table 6: Precoding matrix $\mathbf{C}_k (k = 1, 2, 3, 4)$ for the open-loop spatial multiplexing.

	Number of layers M		
	2	3	4
$\mathbf{C}_1$	$\mathbf{W}_{12}^{\{12\}}/\sqrt{2}$	$\mathbf{W}_{12}^{\{123\}}/\sqrt{3}$	$\mathbf{W}_{12}^{\{1234\}}/2$
$\mathbf{C}_2$	$\mathbf{W}_{13}^{\{13\}}/\sqrt{2}$	$\mathbf{W}_{13}^{\{123\}}/\sqrt{3}$	$\mathbf{W}_{13}^{\{1324\}}/2$
$\mathbf{C}_3$	$\mathbf{W}_{14}^{\{13\}}/\sqrt{2}$	$\mathbf{W}_{14}^{\{123\}}/\sqrt{3}$	$\mathbf{W}_{14}^{\{3214\}}/2$
$\mathbf{C}_4$	$\mathbf{W}_{15}^{\{12\}}/\sqrt{2}$	$\mathbf{W}_{15}^{\{123\}}/\sqrt{3}$	$\mathbf{W}_{15}^{\{1234\}}/2$

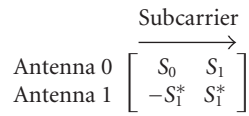

Figure 3: SFBC with two transmit antennas on downlink.

The open-loop spatial multiplexing may be operated when reliable PMI feedback is not available at the eNodeB, for example, when the UE speed is not slow enough or when the feedback overhead on uplink is too high. The open-loop spatial multiplexing with M layers and N transmit antennas ($N \geq M$) is illustrated in Figure 2. The feedback consists of the RI and the CQI in open-loop spatial multiplexing. In contrast to the closed-loop spatial multiplexing, the eNodeB only determines the transmission rank and a fixed set of precoding matrices are applied cyclically across all the scheduled subcarriers in the frequency domain.

The precoding for the open-loop spatial multiplexing mode is defined by

$$\mathbf{y}(i) = \mathbf{W}(i)\mathbf{D}(i)\mathbf{U}\mathbf{x}(i), \tag{2}$$

where $\mathbf{y}(i) = [y_0(i), \ldots, y_{N-1}(i)]^T$, $y_n(i)$ denotes the ith complex symbol transmitted on the nth antenna, the precoding matrix $\mathbf{W}(i)$ is of size $N \times M$, $\mathbf{x}(i) = [x_0(i), \ldots, x_{M-1}(i)]^T$, $x_m(i)$ denotes the ith modulation symbol transmitted on the mth layer, and the DFT precoding matrix $\mathbf{U}$ of size $M \times M$ and the matrix $\mathbf{D}(i)$ of size $M \times M$ supporting the large delay cyclic delay diversity (CDD) are defined in Tables 4 and 5, respectively. When multiple layers are transmitted,

Table 7: Feedback of wideband CQI and subband PMI via PUSCH.

Field	Bit width			
	2 antennas		4 antennas	
	Rank = 1	Rank = 2	Rank = 1	Rank > 1
Rank indicator	1		2	
Wideband CQI for codeword 0	4	4	4	4
Wideband CQI for codeword 1	0	4	0	4
Precoding matrix indication	$2K$	K	$4K$	$4K$

$$\begin{array}{c} \\ \text{Antenna 0} \\ \text{Antenna 1} \\ \text{Antenna 2} \\ \text{Antenna 3} \end{array} \begin{array}{c} \xrightarrow{\text{Subcarrier}} \\ \begin{bmatrix} S_0 & S_1 & 0 & 0 \\ 0 & 0 & S_2 & S_3 \\ -S_1^* & S_0^* & 0 & 0 \\ 0 & 0 & -S_3^* & S_2^* \end{bmatrix} \end{array}$$

Figure 4: SFBC + FSTD with four transmit antennas on downlink.

$\mathbf{D}(i)\mathbf{U}$ effectively makes the modulation symbols of a single codeword are mapped onto different layers for each i in a cyclic manner with period M as the index i increases so that a codeword can experience all the transmitted layers. For two transmit antennas, $\mathbf{W}(i)$ is given by

$$\mathbf{W}(i) = \frac{1}{\sqrt{2}} \begin{bmatrix} 1 & 0 \\ 0 & 1 \end{bmatrix}. \tag{3}$$

For four transmit antennas, to have additional robustness against the spatial channel characteristics, a set of precoding matrices are assigned to $\mathbf{W}(i)$ cyclically as the index i increases according to the followings:

$$\mathbf{W}(i) = \mathbf{C}_k \tag{4}$$

where the index k is given by $k = (\lfloor i/M \rfloor \bmod 4) + 1$ and $\mathbf{C}_k(k = 1, 2, 3, 4)$ for different rank values is given in Table 6. It is noted that in the open-loop spatial multiplexing mode, the transmit diversity scheme is applied when the transmission rank is set to one.

3. Transmit Diversity in LTE

For LTE downlink, the transmit diversity schemes can be applied to all the physical channels such as PDSCH, Physical Broadcast Channel (PBCH), Physical Control Format Indicator Channel (PCFICH), Physical Downlink Control Channel (PDCCH), and Physical Hybrid ARQ Indicator Channel (PHICH) while the other MIMO schemes are only applicable to PDSCH.

A UE can recognize the number of transmit antennas at eNodeB among $\{1, 2, 4\}$ by blindly decoding PBCH, since there is no explicit signaling for it. Note that no transmit diversity scheme applied to the primary and secondary synchronization signals [11] is specified in LTE. Once the number of transmit antennas at eNodeB is detected, a specific transmit diversity scheme applicable to the other physical downlink channels is determined.

Transmit diversity schemes defined for LTE downlink are illustrated in Figures 3, 4, and 5. The space-frequency block code (SFBC) as shown in Figure 3 is used if the eNodeB has two transmit antennas. For the eNodeB with four transmit antennas, a combination of the SFBC and the frequency-switched transmit diversity (FSTD) as shown in Figure 4 is used to provide robustness against the correlation between channels from different transmit antennas and for easier UE receiver implementation. The transmit diversity scheme shown in Figure 4 can be used for all downlink channels other than PHICH. The transmit diversity scheme used for PHICH is shown in Figure 5. In this scheme, four different ACK/NAK bits are multiplexed using orthogonal codes with spreading factor of four over a group of four subcarriers and the resulting group is repeated three times in the frequency domain to achieve frequency diversity gain. To maintain the orthogonality between different codes in each repetition of four subcarriers, antenna switching is not applied within each repetition. Instead, the set of antennas changes across different repetitions as shown in Figure 5. When there are multiple PHICHs transmitted, using type 1 or type 2 alternatively for different PHICHs would be helpful to keep uniform power distribution over eNodeB transmit antennas.

A UE is configured for a transmission scheme such as transmit diversity, SU-MIMO, MU-MIMO, closed-loop rank-1 precoding, and dedicated beamforming when the eNodeB employs multiple transmit antennas. When the eNodeB tries to change the transmission scheme, it may not be possible to transmit the required control message using the configured transmission scheme, for example, SU-MIMO, for the indication of transmission scheme change, since the channel condition is not favorable any longer to the configured transmission scheme. For reliable change of the transmission scheme regardless which transmission scheme is configured for the UE, the transmit diversity can always be used for delivering the required control message to the UE. Hence, the UE shall always try to receive such control message sent using the transmit diversity.

For uplink, the transmit antenna selection diversity for the UE with two transmit antennas is specified. In case of the closed-loop transmit antenna selection, the eNodeB selects the antenna to be used for uplink transmission and communicate this selection to the UE using the downlink control message. For the open-loop transmit antenna selection, the UE autonomously selects the transmit antenna to be used for transmission without eNodeB's intervention. Note that

Type1:

Subcarrier →

Antenna 0	S_0	S_1	S_2	S_3
Antenna 1	0	0	0	0
Antenna 2	$-S_1^*$	S_0^*	$-S_3^*$	S_2^*
Antenna 3	0	0	0	0

1st repetition

Antenna 0	0	0	0	0
Antenna 1	S_0	S_1	S_2	S_3
Antenna 2	0	0	0	0
Antenna 3	$-S_1^*$	S_0^*	$-S_3^*$	S_2^*

2nd repetition

Antenna 0	S_0	S_1	S_2	S_3
Antenna 1	0	0	0	0
Antenna 2	$-S_1^*$	S_0^*	$-S_3^*$	S_2^*
Antenna 3	0	0	0	0

3rd repetition

(a)

Type2:

Subcarrier →

Antenna 0	0	0	0	0
Antenna 1	S_0	S_1	S_2	S_3
Antenna 2	0	0	0	0
Antenna 3	$-S_1^*$	S_0^*	$-S_3^*$	S_2^*

1st repetition

Antenna 0	S_0	S_1	S_2	S_3
Antenna 1	0	0	0	0
Antenna 2	$-S_1^*$	S_0^*	$-S_3^*$	S_2^*
Antenna 3	0	0	0	0

2nd repetition

Antenna 0	0	0	0	0
Antenna 1	S_0	S_1	S_2	S_3
Antenna 2	0	0	0	0
Antenna 3	$-S_1^*$	S_0^*	$-S_3^*$	S_2^*

3rd repetition

(b)

Figure 5: Modified SFBC + FSTD for PHICH with four transmit antennas on downlink.

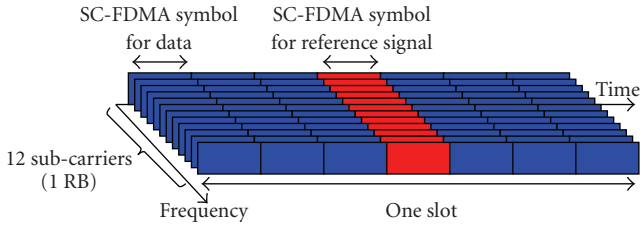

Figure 6: Multiplexing of data and reference signal on uplink.

SFBC-type transmit diversity scheme is not employed for the LTE uplink to avoid additional cost required to implement two power amplifiers at the UE.

4. Closed-loop Rank-1 Precoding in LTE

In the closed-loop rank-1 precoding mode, the eNodeB operates the closed-loop SU-MIMO scheme based on the cell-specific common reference signal with the limitation of selecting a rank-1 precoding matrix for transmission to a UE among the ones defined in Table 1 for two transmit antennas and Table 2 for four transmit antennas to improve data coverage without relying on the UE-specific reference signal. Since the transmission rank is fixed to one in this mode, the related downlink control signaling overhead is smaller than the case of operating the closed-loop SU-MIMO scheme, of which control signaling allows full freedom of selecting the transmission rank among all possible rank values.

5. MU-MIMO in LTE

MU-MIMO scheme is supported in both the uplink and downlink of the LTE standard. In the uplink, the eNodeB can always schedule more than one UEs to transmit in the same time-frequency resource, which forms a MU-MIMO transmission configuration. However, in order for the eNodeB to be able to correctly differentiate and demodulate these UEs' signals, eNodeB needs to assign orthogonal reference signals for these UEs scheduled for the MU-MIMO transmission. Figure 6 shows the uplink slot structure where the reference signal is transmitted using the fourth symbol and the data is transmitted using the others. For a given slot and subframe in each cell, a Zadoff-Chu sequence [11] is defined as the base sequence for uplink reference signals. The cyclically shifted versions of a given Zadoff-Chu sequence form an orthogonal set of sequences. Each UE scheduled for MU-MIMO transmission is assigned a distinctive cyclic shift value, and the UE combines this cyclic shift value with the knowledge of the base Zadoff-Chu sequence to form a reference signal sequence that is orthogonal to other UEs' reference signal sequences. It is noted that the cyclic shift value is always contained in the control signaling, which the UE has to receive for data transmission on uplink, regardless whether the MU-MIMO is operated or not.

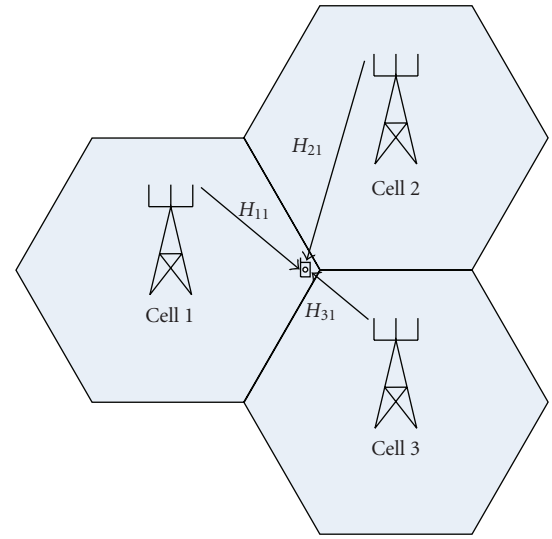

Figure 7: Coordinated multipoint transmission in the downlink.

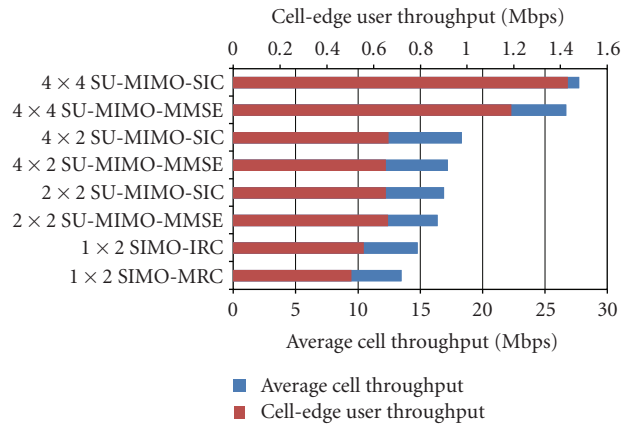

Figure 8: LTE downlink SU-MIMO performance.

In the downlink, if a UE is configured to be in the MU-MIMO transmission mode, only rank-1 transmission can be scheduled to the UE. The eNodeB can schedule multiple UEs, which are configured to be in the MU-MIMO transmission mode, in the same time-frequency resource using different rank-1 precoding matrices from Table 1 for two transmit antennas and Table 2 for four transmit antennas. Note that the UE receives only the information about its own precoding matrix. The scheduled UE then decodes the information data utilizing the common reference signal together with the precoding information obtained from the control signaling. The UE generates the PMI/CQI feedback without any knowledge about other simultaneously scheduled UEs. Hence, there could be mismatch between the UE's CQI report and the actual CQI experienced due to lack of knowledge of interference caused by another UEs scheduled simultaneously. In LTE, for support of receiving higher-order modulation signal such as 16QAM and 64QAM without causing too much complexity in the UE, the transmit power level for each UE is configured in a long-term manner. The per-UE preconfigured power level is hard to maintain in MU-MIMO transmission mode, since eNodeB power amplifier has to support multiple UEs scheduled on the same time-frequency resource. A 1-bit signaling is therefore introduced to indicate whether there is 3 dB power reduction with respect to the per-UE configured power level if a UE is configured in the MU-MIMO transmission mode.

6. Dedicated Downlink Beamforming in LTE

Dedicated beamforming is supported for improving data coverage when the UE supports data demodulation using the UE-specific reference signal. The eNodeB generates a beam using the array of antenna elements (e.g. array of 8 antenna elements), and then applies the same precoding to both the data payload and the UE-specific reference signal with this beam. It is noted that the UE-specific reference signal is transmitted in a way such that its time-frequency location does not overlap with the cell-specific reference signal.

7. Uplink Feedback in LTE

The uplink feedback for support of downlink data transmission consists of the RI, the PMI, and the CQI. The RI indicates the number of layers, which can be accommodated by the current spatial channel experienced at the UE. It was observed in the LTE evaluation that the frequency-selective RI reporting did not provide significant performance benefit, and therefore only one wideband RI is reported for the whole bandwidth. On the contrary, the reporting of PMI and CQI can be either wideband or frequency-selective. The PMI is calculated conditioned on the associated RI, and the CQI is calculated conditioned on the associated RI and PMI. For RI = 1, only one CQI is reported for each reporting unit in frequency, which could be either wideband or subband in the case of frequency-selective report. For RI > 1, CQI for each codeword is reported for the closed-loop spatial multiplexing as different codewords experience different layers, while only one CQI is reported for the open-loop spatial multiplexing as a codeword experiences all layers. The PMI indicates the preferred precoding candidate for the corresponding frequency unit, for example, a particular subband or the whole frequency bandwidth, and is selected from the possible precoding candidates of Table 1 for the case of two transmit antennas and Table 2 for the case of four transmit antennas according to the RI. The CQI indicates the combination of the maximum information data size and the modulation scheme among QPSK, 16QAM, and 64QAM, which can provide block error rate not exceeding 0.1 assuming that the reported rank and the reported precoding matrix are applied in the time-frequency resource. With this definition of CQI, PMI, and RI, the UE can report the maximum data size that it can receive and demodulate, taking into account its receiver ability.

In case of the frequency-selective PMI/CQI reporting, the UE reports a PMI/CQI for each subband. For the non-frequency-selective wideband PMI/CQI reporting, the UE reports a single wideband PMI/CQI corresponding to the whole bandwidth. In the frequency-selective reporting mode, the subband CQI is reported as a differential value with respect to the wideband CQI in order to reduce the signaling overhead. When the frequency-selective CQI reporting is configured, the subband CQIs as well as the wideband CQI is reported, and the wideband CQI serves as the baseline for recovering the downlink channel condition in the whole band.

The frequency-selective report naturally results in large signaling overhead. In the cases where the uplink overhead is a limiting factor, the eNodeB can also configure non-frequency-selective CQI/PMI reports. To cope with various channel conditions and various antenna configurations while keeping the signaling overhead at appropriate level, various feedback modes are specified concerning on the frequency selectivity of the CQI and the PMI reports [13].

The physical channels that can be used for the uplink feedback signaling are Physical Uplink Control Channel (PUCCH) and Physical Uplink Shared Channel (PUSCH). Feedback via PUSCH is used to accommodate large amount

Table 8: Feedback of subband differential CQI and wideband PMI via PUSCH.

Field	Bit width			
	2 antennas		4 antennas	
	Rank = 1	Rank = 2	Rank = 1	Rank > 1
Rank indicator	1		2	
Wideband CQI for codeword 0	4	4	4	4
Subband differential CQI for codeword 0	$2K$	$2K$	$2K$	$2K$
Wideband CQI for codeword 1	0	4	0	4
Subband differential CQI for codeword 1	0	$2K$	0	$2K$
Precoding matrix indication	2	1	4	4

Table 9: Feedback of wideband CQI/PMI via PUCCH.

Field	Bit width			
	2 antennas		4 antennas	
	Rank = 1	Rank = 2	Rank = 1	Rank > 1
Wideband CQI	4	4	4	4
Spatial differential CQI	0	3	0	3
Precoding matrix indication	2	1	4	4

of feedback information in a single reporting instance, since PUSCH is designed for carrying large-size information data packets. For example, the reporting on PUSCH can include the RI, the wideband CQI per codeword, and the PMI for each subband as shown in Table 7, where K is the number of subbands. Note that the rank indicator is separately encoded from the other fields, using one bit for the case of two antennas and two bits for the case of four antennas. The bit width of the other fields is determined according to the rank indicator. Another example is the reporting of the RI, the wideband PMI, the wideband CQI per codeword, and the subband differential CQI for each subband per codeword as shown in Table 8. It is noted that simultaneous reporting of the subband differential CQI and the subband PMI is not supported due to excessive signaling overhead.

PUCCH, on the other hand, is designed for transmission of small amount of control signaling information. Hence, for PUCCH reporting modes, separate time instances are used for reporting the RI, the wideband CQI/PMI, and the subband CQI of the subband selected by the UE. Examples of the wideband CQI/PMI feedback and the subband CQI feedback via PUCCH are shown in Tables 9 and 10, respectively. The spatial differential CQI represents the difference between the CQIs of two codewords and is defined for both the wideband CQI and the subband CQI. In case of the subband CQI feedback, each reporting instance corresponds to a group of subbands, from which the UE selects the subband with best CQI. Due to these characteristics, the eNodeB may configure periodic reporting of limited amount of feedback information on PUCCH, while triggering the UE to report large amount of detailed feedback information on PUSCH if accurate channel information is needed for transmission of large amount of data in the downlink.

8. MIMO Schemes in LTE-Advanced

In order to support downlink peak spectrum efficiency of 30 bps/Hz and uplink peak spectrum efficiency of 15 bps/Hz according to LTE-Advanced requirement [14], the spatial multiplexing with antenna configuration of 8×8 for downlink transmission and 4×4 for uplink transmission is being investigated. Here $N \times N$ denotes a configuration of N transmit antennas and N receive antennas.

In addition to meeting the peak spectrum efficiency, further improvement of the average cell throughput as well as the cell edge performance is also an important aspect of the LTE-advanced study. Coordinated multipoint transmission/reception is a candidate technology where antennas of multiple cell sites are utilized in a way such that the transmit/receive antennas of the serving cell as well as the neighboring cells can contribute in improving quality of the received signal at the UE/eNodeB, as well as in reducing the cochannel interferences from neighboring cells. The application of coordinated multipoint transmission is illustrated in Figure 7 for a downlink transmission scenario. An example scheme is to form a beam to the scheduled UE by using the transmit antennas of the cells 1, 2, and 3, where each cell transmits the same data to the scheduled UE and the UE-specific reference signal is used for support of demodulation at the UE. For the cells 1, 2, and 3 to jointly form the transmit signal matching to the composite channel experienced by the UE, it may be necessary to provide feedback representing the downlink spatial channel of each cell without any preassumption on operation at the eNodeB transmitter and the UE receiver. The feedback for explicit representation of the spatial channel of each cell may naturally require much larger overhead than the feedback defined in LTE such as CQI, PMI, and RI.

Table 10: Feedback of subband CQI via PUCCH.

Field	Bit width			
	2 antennas		4 antennas	
	Rank = 1	Rank = 2	Rank = 1	Rank > 1
Subband CQI	4	4	4	4
Spatial differential CQI	0	3	0	3
Subband label	1 or 2	1 or 2	1 or 2	1 or 2

Other areas for further investigation in LTE-Advanced are for example as follows:

(i) further enhancement of downlink MU-MIMO to improve the system throughout beyond what was achieved in LTE;

(ii) introduction of uplink transmit diversity utilizing up to four transmit antennas;

(iii) extension of downlink transmit diversity to eight transmit antennas;

9. Performance Evaluation

Figure 8 shows the LTE downlink SU-MIMO performance in terms of average cell throughput and cell-edge user throughput obtained by system level simulation, where $N \times L$ represents the configuration of N eNodeB transmit antennas and L UE receive antennas. Simulation parameters and assumptions follow the guideline provided in [2]. Linear antenna arrays with antenna spacing 10λ are assumed for eNodeB transmit antennas, where λ denotes the wavelength of the carrier frequency. The results in Figure 8 are for Case 1 representing interference-limited small urban macrocell environments, where the carrier frequency is 2 GHz, the inter-site distance is 500 m, the bandwidth is 10 MHz, and the UE speed is 3 km/h. The 2-tier cell layout with 57 cells in total was considered and 10 users were dropped per cell.

For single input multiple output (SIMO), two linear receiver methods are used: maximal ratio combining (MRC) and interference rejection combining (IRC). For SU-MIMO, MMSE and MMSE with successive interference cancellation (MMSE-SIC) receivers are used. Since IRC and SIC are designed to reduce or cancel the interference, they outperform MRC and MMSE, respectively, which are designed considering the desired signals only.

The simulation results for the antenna configurations of 2×2 and 4×4 show how much the spatial multiplexing scheme introduced in LTE improves the system level performance. Comparing MIMO-SIC with SIMO-IRC, we observe 14% and 87% gain from 2×2 and 4×4, respectively, in terms of average cell throughput.

In the antenna configuration of 4×2, up to 2 layers can be constructed using the precoding schemes designed for 4 transmit antennas. Comparing the performance between the antenna configurations of 4×2 and 2×2, we can observe the precoding gain with more transmit antennas. The results in Figure 8 show that 4×2 configuration provides 8.2% gain over 2×2 configuration in terms of average cell throughput.

It is also observed from the results in Figure 8 that the MIMO technologies introduced in LTE successfully improve the cell-edge user throughputs.

10. Conclusion

In this paper, we introduced MIMO features of LTE, which are downlink SU-MIMO, transmit diversity, closed-loop rank-1 precoding, MU-MIMO, dedicated beamforming, and further described technical backgrounds for specifying those technologies. Uplink feedback mechanisms for support of downlink MIMO technologies were also described to provide better understanding about LTE system operation. In addition, the MIMO schemes being studied for LTE-Advanced were briefly described.

References

[1] I. E. Telatar, "Capacity of multi-antenna Gaussian channels," *European Transactions on Telecommunications*, vol. 10, no. 6, pp. 585–595, 1995.

[2] 3GPP, TR 25.814, "Physical layer aspects for evolved Universal Terrestrial Radio Access (Release 7)".

[3] G. Foschini and M. J. Gans, "On the limits of wireless communications in a fading environment when usingmultiple atnennas," *Wireless Personal Communications*, vol. 6, no. 3, pp. 311–355, 1998.

[4] D. Agrawal, V. Tarokh, A. Naguib, and N. Seshadri, "Space-time coded OFDM for high data-rate wireless communication over wideband channels," in *Proceedings of the 48th IEEE Vehicular Technology Conference (VTC '98)*, vol. 3, pp. 2232–2236, Ottawa, Canada, 1998.

[5] H. El Gamal and M. O. Damen, "An algebraic number theoretic framework for space-time coding," in *Proceedings of IEEE International Symposium on Information Theory*, p. 132, Lausanne, Switzerland, June-July 2002.

[6] B. Hassibi and B. M. Hochwald, "High-rate codes that are linear in space and time," *IEEE Transactions on Information Theory*, vol. 48, no. 7, pp. 1804–1824, 2002.

[7] N. Al-Dhahir and A. H. H. Sayed, "The finite-length multi-input multi-output MMSE-DFE," *IEEE Transactions on Signal Processing*, vol. 48, no. 10, pp. 2921–2936, 2000.

[8] H. Bölcskei, D. Gesbert, and A. J. Paulraj, "On the capacity of OFDM-based spatial multiplexing systems," *IEEE Transactions on Communications*, vol. 50, no. 2, pp. 225–234, 2002.

[9] http://www.3gpp.org.

[10] 3GPP, TS 36.201, "Evolved Universal Terrestrial Radio Access (E-UTRA); LTE Physical Layer-General Description (Release 8)".

[11] 3GPP, TS 36.211, "Evolved Universal Terrestrial Radio Access (E-UTRA); Physical Channels and Modulation (Release 8)".

[12] 3GPP, TS 36.212, "Evolved Universal Terrestrial Radio Access (E-UTRA); Multiplexing and channel coding (Release 8)".
[13] 3GPP, TS 36.213, "Evolved Universal Terrestrial Radio Access (E-UTRA); Physical layer procedures (Release 8)".
[14] 3GPP, TR 36.913, "Requirements for Further Advancements for E-UTRA (LTE-Advanced) (Release 8)".
[15] 3GPP, TR 36.814, "Further Advancements for E-UTRA; Physical Layer Aspects".
[16] 3GPP, TS 36.306, "Evolved Universal Terrestrial Radio Access (E-UTRA); User Equipment (UE) radio access capabilities (Release 8)".
[17] G. H. Golub and C. F. Van Loan, *Matrix Computations*, The Johns Hopkins University Press, Baltimore, Md, USA, 1996.

EURASIP Journal on Wireless Communications and Networking

Special Issue on
Physical Layer Network Coding for Wireless Cooperative Networks

Call for Papers

Cooperative communication is an overwhelming research topic in wireless networks. The notion of cooperative communication is to enable transmit and receive cooperation at user level by exploiting the broadcast nature of wireless radio waves so that the overall system performance including power efficiency and communication reliability can be improved. However, due to the half-duplex constraint in practical systems, cooperative communication suffers from loss in spectral efficiency. Network coding has recently demonstrated significant potential for improving network throughput. Its principle is to allow an intermediate network node to mix the data received from multiple links for subsequent transmission. Applying the principle of network coding to wireless cooperative networks for spectral efficiency improvement has recently received tremendous attention from the research community. *Physical-layer network coding* (PLNC) is now known as a set of signal processing techniques combining channel coding, signal detection, and network coding in various relay-based communication scenarios, such as two-way communication, multiple access, multicasting, and broadcasting. To better exploit this new technique and promote its applications, many technical issues remain to be studied, varying from fundamental performance limits to practical implementation aspects. The aim of this special issue is to consolidate the latest research advances in physical-layer network coding in wireless cooperative networks. We are seeking new and original contributions addressing various aspects of PLNC. Topics of interest include, but not limited to:

- Fundamental limits of relay channels with PLNC
- Protocol design and analysis for PLNC
- Cross-layer design for systems with PLNC
- Joint channel coding, modulation, and PLNC
- PLNC with Turbo/LDPC codes
- PLNC with fountain codes
- Channel estimation and synchronization of PLNC
- Scheduling and resource allocation with PLNC
- PLNC with MIMO and OFDM
- PLNC in cooperative and cognitive networks
- Implementation aspects of PLNC
- Random network coding
- Other issues related to PLNC

Before submission authors should carefully read over the journal's Author Guidelines, which are located at http://www.hindawi.com/journals/wcn/guidelines.html. Prospective authors should submit an electronic copy of their complete manuscript through the journal Manuscript Tracking System at http://mts.hindawi.com/ according to the following timetable:

Manuscript Due	January 1, 2010
First Round of Reviews	April 1, 2010
Publication Date	July 1, 2010

Lead Guest Editor

Wen Chen, Department of Electronic Engineering, Shanghai Jiaotong University, Minhang, Shanghai, China; wenchen@sjtu.edu.cn

Guest Editors

Xiaodai Dong, Department of Electrical and Computer Engineering, University of Victoria, BC, Canada; xdong@ece.uvic.ca

Pingyi Fan, Department of Electronic Engineering, Tsinghua University, Beijing, China; fpy@mail.tsinghua.edu.cn

Christoph Hausl, Institute for Communications Engineering, Technische Universität München, Germany; christoph.hausl@tum.de

Tiffany Jing Li, Department of Electrical and Computer Engineering, Lehigh University, Bethlehem, PA 18015, USA; jingli@ece.lehigh.edu

Petar Popovski, Department of Electronic Systems, Aalborg University, Niels Jernes Vej 12, 5-208 9220 Aalborg, Denmark; petarp@es.aau.dk

Meixia Tao, Department of Electronic Engineering, Shanghai Jiaotong University, Minhang, Shanghai, China; mxtao@sjtu.edu.cn

EURASIP Journal on Bioinformatics and Systems Biology

Special Issue on
Computational Approaches to Assist Disease Mechanism Discovery

Call for Papers

Rapidly advanced biotechnology has created a number of "omics" such as genomics, transcriptomics, proteomics, and epigenomics. This massive biological data provides new perspectives on disease study. Many computational algorithms have been proposed and implemented to extract information from diverse data resources in order to characterize human diseases and develop treatment strategies. However, most of the proposed methodologies have still not achieved the sensitivity and specificity to be effectively used.

The main focus of this Special Issue will be on the study of diseases through computational approaches. How to integrate large-scale biological data and clinical data to understand disease physiology and pathology, and to advance disease diagnosis and treatment? We invite authors to present original research articles as well as review articles that will stimulate the continuing efforts in computational study of disease mechanisms. Potential topics include, but are not limited to:

- Machine learning application in disease data analysis
- Pattern recognition in disease data
- Methods to identify disease genes and pathways
- System approaches to discover drug target or diagnostic biomarker
- SNP, protein structure, and diseases
- Phenome-Genome integrative approach for disease study

Besides, only papers with strong validation methodology will be selected. In addition, papers where the methods have been demonstrated in the clinic to deliver a diagnostic, prognostic, or therapeutic choice of value will be preferred. Before submission authors should carefully read over the journal's Author Guidelines, which are located at http://www.hindawi.com/journals/bsb/guidelines.html. Prospective authors should submit an electronic copy of their complete manuscript through the journal Manuscript Tracking System at http://mts.hindawi.com/ according to the following timetable:

Manuscript Due	January 1, 2010
First Round of Reviews	April 1, 2010
Publication Date	July 1, 2010

Lead Guest Editor

Haiyan Hu, School of Electrical Engineering and Computer Science, University of Central Florida, Orlando, FL 32875, USA; haihu@cs.ucf.edu

Guest Editors

Mehmet Dalkilic, School of Informatics, Indiana University, Bloomington, IN, USA; dalkilic@indiana.edu

Gary Livingston, Computer Science Department, University of Massachusetts Lowell, Lowell, MA, USA; gary@cs.uml.edu

Alison A. Motsinger-Reif, Bioinformatics Research Center, Department of Statistics, North Carolina State University, Raleigh, NC, USA; motsinger@stat.ncsu.edu

Motoki Shiga, Laboratory of Pathway Engineering, Bioinformatics Center, Institute for Chemical Research, Kyoto University, Kyoto, Japan; shiga@kuicr.kyoto-u.ac.jp

EURASIP Journal on Wireless Communications and Networking

Special Issue on High-Throughput Wireless Baseband Processing

Call for Papers

Wireless communications is a fast-paced area, where many standards, protocols, and services are introduced each year. Implementation of every new standard becomes challenging especially when more and more higher data rates up to several gigabits/second are required. On the other hand, the power budget is not increasing in the same pace. The presence of all those different modes as well as high throughput requirements brought the need for designing almost-all-digital radios, which benefit from technology scaling. Those goals can only be achieved by efficient algorithms, models, and methods for the design of high-throughput and low-power systems for baseband processing. This special issue will report the recent advances of very high throughput and low-power systems for wireless baseband processing. Areas of interest include, but are not limited to:

- Modeling of quality-of-service, reliability, and performance in high-throughput wireless systems
- Power-aware and/or low-cost algorithms and architecture optimizations for multistandard baseband processing
- Baseband compensation techniques for RF/analog circuit impairments
- High-throughput baseband processing for software-defined and cognitive radios
- Applications to WirelessHD, IEEE 802.15.3c, MIMO systems, UWB, WiMAX, and LTE systems

Before submission authors should carefully read over the journal's Author Guidelines, which are located at http://www.hindawi.com/journals/wcn/guidelines.html. Prospective authors should submit an electronic copy of their complete manuscript through the journal Manuscript Tracking System at http://mts.hindawi.com/ according to the following timetable:

Manuscript Due	October 1, 2009
First Round of Reviews	January 1, 2010
Publication Date	April 1, 2010

Lead Guest Editor

Taskin Kocak, University of Bristol, Bristol, UK; t.kocak@bristol.ac.uk

Guest Editors

Mustafa Badaroglu, ON Semiconductor Vilvoorde, Belgium; mustafa.badaroglu@onsemi.com

Dake Liu, Linkoping University, Linkoping, Sweden; dake@isy.liu.se

Liesbet Van der Perre, IMEC, Leuven, Belgium; vdperre@imec.be